



HAL
open science

Gut microbiota analysis for prediction of clinical relapse in Crohn's disease

Sylvie Buffet-Bataillon, Guillaume Bouguen, François Fleury, Vincent Cattoir,
Yann Le Cunff

► **To cite this version:**

Sylvie Buffet-Bataillon, Guillaume Bouguen, François Fleury, Vincent Cattoir, Yann Le Cunff. Gut microbiota analysis for prediction of clinical relapse in Crohn's disease. *Scientific Reports*, 2022, 12 (1), pp.19929. 10.1038/s41598-022-23757-x . hal-03868943

HAL Id: hal-03868943

<https://hal.science/hal-03868943v1>

Submitted on 23 Jan 2023

HAL is a multi-disciplinary open access archive for the deposit and dissemination of scientific research documents, whether they are published or not. The documents may come from teaching and research institutions in France or abroad, or from public or private research centers.

L'archive ouverte pluridisciplinaire **HAL**, est destinée au dépôt et à la diffusion de documents scientifiques de niveau recherche, publiés ou non, émanant des établissements d'enseignement et de recherche français ou étrangers, des laboratoires publics ou privés.



Distributed under a Creative Commons Attribution 4.0 International License



OPEN

Gut microbiota analysis for prediction of clinical relapse in Crohn's disease

Sylvie Buffet-Bataillon¹, Guillaume Bouguen², François Fleury¹, Vincent Cattoir³ & Yann Le Cunff⁴✉

The role of intestinal bacterial microbiota has been described as key in the pathophysiology of Crohn's disease (CD). CD is characterized by frequent relapses after periods of remission which are not entirely understood. In this paper, we investigate whether the heterogeneity in microbiota profiles in CD patients could be a suitable predictor for these relapses. This prospective observational study involved 259 CD patients, in which 41 provided an additional total of 62 consecutive fecal samples, with an average interval of 25 weeks in between each of these samples. Fecal microbiota was analyzed by massive genomic sequencing through 16 S rRNA amplicon sampling. We found that our 259 CD patients could be split into three distinct subgroups of microbiota (G1, G2, G3). From G1 to G3, we noticed a progressive decrease in alpha diversity ($p \leq 0.0001$) but no change in the fecal calprotectin (FC) level. Focusing on the 103 consecutive samples from 41 CD patients, we showed that the patients microbiota profiles were remarkably stable over time and associated with increasing symptom severity. Investigating further this microbiota/severity association revealed that the first signs of aggravation are (1) a loss of the main anti-inflammatory Short-Chain Fatty Acids (SCFAs) *Roseburia*, *Eubacterium*, *Subdoligranumum*, *Ruminococcus* ($P < 0.05$), (2) an increase in pro-inflammatory pathogens *Proteus*, *Finexgoldia* ($P < 0.05$) while (3) an increase of other minor SCFA producers such as *Ezakiella*, *Anaerococcus*, *Megasphaera*, *Anaeroglobus*, *Fenollaria* ($P < 0.05$). Further aggravation of clinical signs is significantly linked to the subsequent loss of these minor SCFAs species and to an increase in other proinflammatory Proteobacteria such as *Klebsiella*, *Pseudomonas*, *Salmonella*, *Acinetobacter*, *Hafnia* and proinflammatory Firmicutes such as *Staphylococcus*, *Enterococcus*, *Streptococcus*. ($P < 0.05$). To our knowledge, this is the first study (1) specifically identifying subgroups of microbiota profiles in CD patients, (2) relating these groups to the evolution of symptoms over time and (3) showing a two-step process in CD symptoms' worsening. This paves the way towards a better understanding of patient-to-patient heterogeneity, as well as providing early warning signals of future aggravation of the symptoms and eventually adapting empirically treatments.

Crohn's disease (CD) is characterized by chronic inflammation of the gastrointestinal (GI) tract, which involves complex interactions between the host immune system, intestinal mucosa and gut microbiota¹. Numerous studies have found an imbalance in the gut microbiota of CD patients compared to non-CD controls with an overall loss of diversity, a depletion of firmicutes and an increase in Proteobacteria²⁻⁴. The chronic, unpredictable nature of the disease and its debilitating effect on all aspects of life are major concerns for patients with CD with a broad diversity of symptoms^{5,6}. For instance, 21–47% of CD patients present in addition to digestive symptoms, systemic and extra-intestinal manifestations⁷. Half of CD patients develop intestinal complications, such as strictures or fistulae, within 10 years of diagnosis and require surgery in the 20 years following the diagnosis^{8,9}. In a nutshell, it is well documented that CD displays a large heterogeneity of symptoms between patients—from mild to heavily impairing everyday life -, as well as in time with a relapsing–remitting dynamics that is also yet to be fully understood. It is also still unclear how such inter-patient heterogeneity in symptoms and CD evolution is associated with microbiota heterogeneity. In this paper, we harness a novel large longitudinal cohort of Crohn's patients to unravel this relationship.

¹INSERM, Institut NUMECAN (Nutrition Metabolisms and Cancer), CHU Rennes, Université Rennes 1, 35000 Rennes, France. ²CIC 1414, INSERM, Institut NUMECAN (Nutrition Metabolisms and Cancer), CHU Rennes, Université Rennes 1, 35000 Rennes, France. ³U1230, INSERM, CHU Rennes, Université Rennes 1, 35000 Rennes, France. ⁴Dyliss - Dynamics, Logics and Inference for biological Systems and Sequences, Inria Rennes – Bretagne Atlantique, Université Rennes 1, Rennes, France. ✉email: yann.lecunff@univ-rennes1.fr

	CD patients [(n = 259)/(n = 41)]
Age (mean ± SD)	41 ± 15/45 ± 15
Female sex (%)	145 (56%)/20 (49%)
Smoking (%)	43 (25%)/9 (22%)
Gastrointestinal surgery	54 (21%)/14 (34%)
Montreal A (%)	A1: 35 (19%)/4 (10%); A2: 124 (68%)/30 (77%); A3: 23 (13%)/5 (13%)
Montreal B (%)	B1: 111 (62%)/23 (61%); B2: 39 (22%)/10 (26%); B3: 29 (16%)/5 (13%)
Montreal L (%)	L1: 54 (29%)/10 (25%); L2: 31(17%)/7 (18%); L3: 99(54%)/23 (57%)
Fecal calprotectin (µg/g), median (IQR)	122.5 (31.75–529.75)/322 (72–531.5)
Anti-TNF (%)	154 (59%)/34 (83%)
Thiopurines (%)	126 (48%)/28 (68%)
MTX (%)	141 (54%)/8 (20%)

Table 1. Characteristics of the cohort (n = 259 patients/n = 41 patients). Montreal A (age at diagnosis): A1: < 16 years; A2: 17–40 years; and A3: > 40 years. Montreal L (disease location): L1 ileum; L2 colon; L3 ileum–colon. Montreal B (disease behavior): B1 inflammatory; B2 structuring; B3 penetrating. Anti-TNF: infliximab, adalimumab, ustekinumab, vedolizumab. Thiopurines: azathioprine, 6-mercaptopurine. CD Crohn's disease, MTX methotrexate.

We thus investigated (1) the heterogeneity of gut microbiota in CD patients, (2) for the first time the temporal evolution of the disease in order to link symptoms' evolution and microbiota composition, and (3) the “key microbial signatures” during the transitions from one microbiota profile to another in order to pave the way towards personalized diagnosis and treatment of CD.

Methods

Cohort of patients. A total of 259 patients with CD were included at the referral center Hospital University of Rennes (France) during a two-year period and provided informed consent for this observational, non-interventional study. Patients were informed to be included in a prospective research database (Rennes, approved by the Commission Nationale Informatique et Liberté (CNIL) No. 1412467) which allowed us to perform this study without additional consent as the data were retrieved from the standard follow-up of patients.

Inclusion criteria were CD patients diagnosed using standard endoscopic, histological or radiological criteria, aged from 16 to 80 years old. Exclusion criteria were patients with ulcerative colitis, and/or with a stoma. Details regarding age, female sex, smoking, gastrointestinal surgery, Montreal classification for CD (A, B, L), fecal calprotectin (FC)(µg/g), treatment (Anti-TNF, Thiopurine-methotrexate (MTX), Antibiotics) were collected on the same day of fecal samples and are shown in Table 1.

Patient selection. A subgroup of 41 patients from the cohort had several temporal fecal samplings over the longitudinal study (n = 103 samples in total). The Harvey-Bradshaw Index (HBI) was assessed to describe the status of a patient at the time when the sample was taken. HBI thresholds were used to define three groups “Remission” (HBI < 5 with abdominal pain = 0 and complications = 0) (n = 42); “Mild-Moderate” (HBI = 5–8 with abdominal pain = 1 (mild) or 2 (moderate) and complications = 0) (n = 28); and “Severe” (HBI > 8 with abdominal pain = 3 and at least one complications) (n = 33)¹⁰.

Gut microbiota analysis. We used a standard procedure for fecal microbiota profiling using 16S rRNA-based metagenomic sequencing and bioinformatic analysis. According to the International Human Microbiome Standards (IHMS), patients were asked to collect fecal samples immediately after defecation in a sterile container (from VWR). Then, the stool samples were stored up to 24 h at 4 °C. When received at the laboratory, all samples were manually homogenized and weighed into separate aliquots for storage at 80 °C until DNA extraction.

The extracted DNA was used for the assessment of the microbial populations using 16S rRNA gene sequence-based microbiota analysis. DNA was extracted from the fecal specimens with the automated MagNA Pure system (Roche Diagnostics GmbH, Mannheim, Germany), using the MagNA Pure LC DNA Kit III (bacteria, fungi) (Roche) according to the manufacturer's recommendations. Pre-isolation steps as mechanical lysis (30 s at 6000 rpm) on the MagNa Lyser Instrument, and heat lysis (10 min at + 65 °C and at 95 °C) were added to perform DNA isolations.

We followed the steps described in the Illumina 16S sample preparation guide to amplify the V3 and V4 region, add Illumina sequencing adapters and dual index barcodes to the amplicon target.

Primers were designed according to the V3-V4 regions of bacteria (the upstream primer: PCR_341 F is 5'-CCTACGGGNGGCWGCAG-3', and the downstream primer: PCR_785R is 5'-GACTACHVGGGTATCTAATCC-3')¹¹. The Illumina overhang adapter sequences used were as follows: Forward overhang: 5' TCGTCG GCACGTCAGATGTGTATAAGAGACAG-[PCR_341F]; Reverse overhang: 5' GTCTCGTGGGCTCGGAGATGTGTATAAGAGACAG-[PCR_785R].

Primers linked to adapters were used for PCR amplification; the PCR products were purified, quantified, and then normalized to form a sequencing library. These were sequenced by Illumina MiSeq as outlined in the Illumina 16S sample preparation guide.

The individual sequence reads obtained were filtered, trimmed and processed as described by Escudie and al. according to Find Rapidly OTUs with Galaxy Solution (FROGS)¹². All reads were classified to the lowest possible taxonomic level (species or genus) using FROGS. The SILVA database used for taxonomic assignment was SILVA 16S v132 A table of 16S rRNA Operational Taxonomic Units (OTUs) was then generated.

Statistical analysis. For the clustering of microbiota profiles, we performed the following procedure. First, the clr transform was applied to the OTU count table (patients in row, OTU labels in column) from the R phyloseq package (v1.32.0), similar to Tsilimigras et al.¹³. This table was then normalized to achieve a mean of 0 and a standard deviation of 1 per column, akin to the first step of performing a Principal Component Analysis (PCA)¹⁴. The non-supervised clustering used is an Ascending Hierarchical Clustering, with a euclidean distance and the Ward aggregation method (sciPy Python package, v1.8.1)¹⁵. As we opted for a non-supervised approach, we did not use a train/test split, which would have been required if we had to train a model to predict the severity of the symptoms. The PCA analysis and the Silhouette computation to assess the number of clusters were performed in Python with the package scikit-learn (sklearn). The highest silhouette coefficient identified two distinct groups and the second highest identified three groups.

To assess alpha diversity, the Chao1 and Shannon diversity indices were used. To investigate whether dysbiosis could be linked to inflammation, we tested whether fecal calprotectin levels would vary between groups of microbiota, using a Kruskal–Wallis test. Then, to estimate the temporal evolution of dysbiosis, groups identified by hierarchical clustering were assessed with respect to symptoms' severity using Fisher's exact test. Finally, to identify the “key microbial signatures” in the dynamics of the disease, the differential abundance of species between patients was determined using DESeq2 and apglm packages with p-value adjusted for multiple testing using the Benjamini–Hochberg method (cut-off = adjusted $p < 0.05$). Since confounding factors may influence the fecal microbiome^{7,16,17} and to feel confident in the relevant changes in bacterial groups observed in our study, we also quantified the influence of known factors as smoking and disease localization on the three groups of microbiota. Statistical analysis and data visualizations were performed using R (v.3.5.1) with multiple packages, including ‘phyloseq’ (v1.32.0), ‘philir’ (v1.14.0), ‘ggplot 2’ (v3.3.6), ‘grid’ (v4.1.3), ‘ape’ (v4.1), ‘scales’ (v1.2.0), ‘DESeq 2’ (v1.28.1) and ‘apglm’ (v1.1.16 from BiocManager v1.30.18).

Ethics approval and consent to participate. The study was carried out in accordance with national guidelines and authority regulations for research. All experimental protocols were approved by a named institutional review board and/or licensing ethics committee. Patients were informed to be included in a prospective research database (Rennes, Commission Nationale Informatique et Liberté (CNIL) No. 1412467) that allowed us to perform study without additional consent as the data were retrieved from the standard of care follow-up of patients.

Results

Characteristics of CD patients. The characteristics of the 259 patients and 41 patients with CD are summarized in Table 1. More than 80% of the cohort displays inflammation in the lower part of the gut. Only two of the 259 patients (0.08%) received antibiotics (metronidazole or ciprofloxacin) within 90 days of microbiota analysis. As the data retrieved from the standard follow-up of patients, the timing between consecutive samples and the total number of samples collected differed between the 41 patients. Precisely, 26 patients had 2 samples, 9 patients had 3 and 6 patients had 4. The median time interval between two samples was 15 weeks and the average time interval was 25 weeks.

Three distinct groups of microbiota profiles in CD patients. Of the 321 gut microbiota samples analyzed from 259 patients, our clustering method identified three groups of microbiota profiles (G1, G2 and G3) that significantly differed in terms of gut microbiota (Fig. 1A). Species diversity was found to decrease from G1 to G2 and from G2 to G3, based on Chao1 and Shannon indexes (Fig. 1B) (Kruskal–Wallis test, $p = 4.02e-13$ and $2.6e-15$, respectively). The analysis of the gut microbiota showed significant changes in the proportion of the microbial phyla Proteobacteria between G1, G2 and G3 groups (Fig. 1C) (Fisher exact test, $p < 0.05$). No association between confounding factors such as smoking or disease localization and the three groups of microbiota was found. Interestingly, while the three groups displayed a broad diversity of microbiota, they did not display significant differences in terms of calprotectin levels (Fig. 1D, Kruskal–Wallis test, $p = 0.26$).

Dynamics of fecal bacterial clustering in CD Patients over time. We then focused on the subset of 41 patients with multiple microbiota samples (from 2 to 4 samples per individual), which represented 103 samples overall. In Fig. 2A, we show a strong association between microbiota composition and symptoms severity (Fisher's exact test, $p = 3.46e-06$): G3 was mainly associated to “Severe” CD cases [20/27 (74%)]; G2 to “Remission” CD cases [18/39 (46.1%)] as well as to “Mild-Moderate” CD cases [15/39 (38.5%)]; and finally, G1 to “Remission” CD cases [21/37 (56%)]. Figure 2B displays the three groups in the Principal Component Analysis (PCA) plan, that is, a 2D projection of the patients' microbiota. One can notice that G2 is positioned between G1 and G3, in agreement with the increase of symptoms severity from G1 to G3. In Fig. 2C, we show the transitions between groups from two successive medical appointments. No transitions from G1 to G3 and only two transitions from G3 to G1 were observed. Moreover, every observed improvement in terms of symptoms was associated with either a stability of the microbiota group or a transition either from G3 to G2 or from G2 to G1

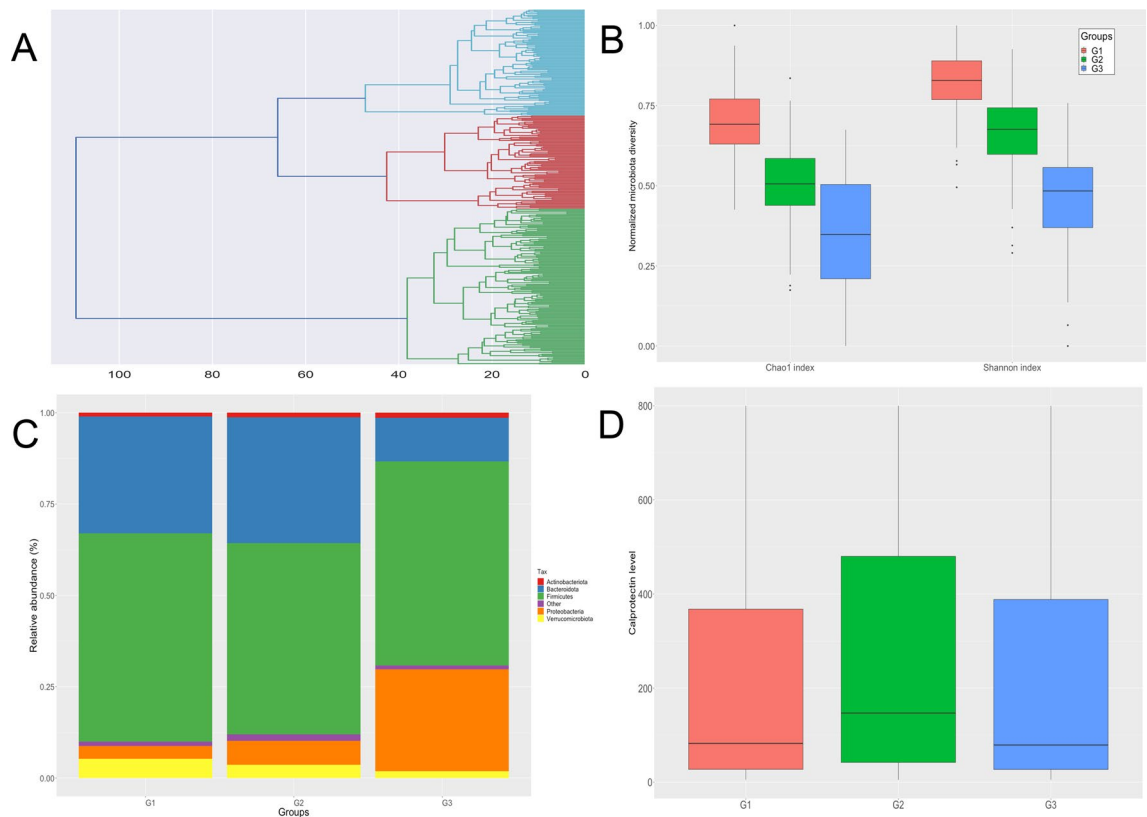


Figure 1. Gut microbiota from 259 CD patients ($n = 321$ samples). **(A)** Ascending hierarchical classification (AHC) of the 321 gut microbiota: three distinct groups (G1, G2, G3) are identified, depicted in blue, red and green, respectively. **(B)** A decreasing Shannon index and Chao1 index is observed from G1 to G3 ($p = 2.6 \times 10^{-15}$ and 4.02×10^{-13} respectively). **(C)** Global composition of gut microbiota at the phyla level in G1, G2 and G3. **(D)** Association between the three groups of gut microbiota G1, G2 and G3 and Calprotectin levels in CD patients: Calprotectin levels are not significantly different between G1, G2 and G3, despite differences in degree of dysbiosis.

($n = 15/15$). As such, our results hint that the more common transitions from G1 to G2 or from G2 to G3 could be key indicators of the disease's evolution over time.

Key microbial signatures to predict changes in CD symptoms over time. We then investigated in more detail the “key microbial signatures” i.e. the difference between G1, G2 and G3 microbiota profiles, as they result in different dynamics of the disease.

Figure 2D shows that the first sign of aggravation (transition from G1 to G2) is threefold: (1) a decrease of the main anti-inflammatory microorganisms belonging to the main SCFA-producing bacteria (*Roseburia*, *Eubacterium*, *Subdoligranulum*, *Ruminococcus*) ($p < 0.05$), (2) an increase in pro-inflammatory pathogens (*Proteus*, *Finegoldia*) ($p < 0.05$) and (3) an increase of minor SCFA producers (*Ezakiella*, *Anaerococcus*, *Megasphaera*, *Anaeroglobus*, *Fenollaria*) ($p < 0.05$). Further aggravation of clinical signs (transition from G2 to G3) (Fig. 2E) is significantly linked (1) to a deeper loss of the minor SCFA-producing bacteria ($p < 0.05$) and (2) to an increase in other pro-inflammatory Proteobacteria (such as *Klebsiella*, *Pseudomonas*, *Salmonella*, *Acinetobacter*, *Hafnia*) and pro-inflammatory Firmicutes (such as *Staphylococcus*, *Enterococcus*, *Streptococcus*) ($p < 0.05$).

Discussion

In this study, we focused on characterizing the microbiota heterogeneity in CD patients in order to better understand the clinical evolution of the disease, rather than the traditional comparison between CD and controls or between CD and other IBDs^{18–25}. We also took advantage of longitudinal information. Indeed, it has been shown that longitudinal profiling of multi-omics datasets even from smaller cohorts have higher performance and information richness than larger cohorts without longitudinal profiling. This has been demonstrated in other complex diseases such as diabetes and obesity^{26,27}. Finally, we decided to take advantage of non-supervised clustering techniques of microbiota in order to shed light on inter-patient heterogeneity, as advocated in recent reviews concerning microbiota analysis^{14,28,29}.

We showed that CD is characterized by three groups of microbiota profiles, G1 being akin to normobiosis in terms of species diversity while G2 and G3 display some form of dysbiosis. In agreement with others, dysbiosis was characterized by a marked reduction in bacteria belonging to the SCFA-producing bacteria of the phylum Firmicutes and an increased presence of the phylum Proteobacteria^{19,22,30–33}.

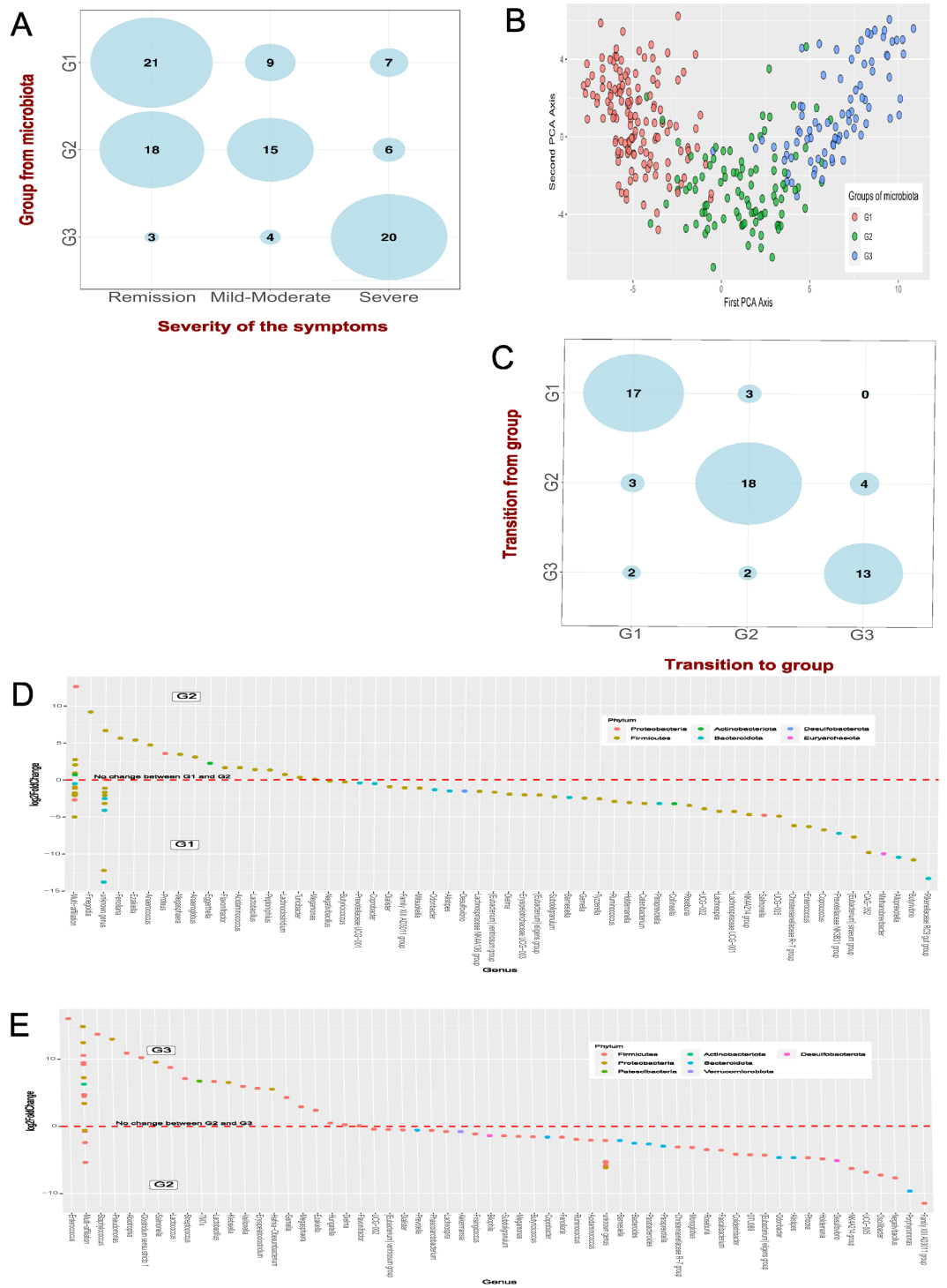


Figure 2. Gut microbiota from 41 CD patients (n = 103 several consecutive samples). **(A)** Association between the groups of gut microbiota G1, G2 and G3 and severity of the symptoms in CD patients. From the groups G1 to G3, an increase in symptoms severity is observed ($p = 3.46 \times 10^{-6}$). **(B)** Projection of the three groups of gut microbiota G1, G2 and G3 with principal component analysis (PCA): G1, G2 and G3 are represented by three different colors. **(C)** Transition of the three groups of gut microbiota G1, G2 and G3 between two consecutive samples: overall, CD patients remain in the same group over time. **(D)** Significant ($p < 0.05$) log-fold changes in the abundances of bacterial species in G2 compared to G1. Positive log-fold change points out an increase in abundance in G2 compared to G1, while negative log-fold change points out a reduction in abundance. **(E)** Significant ($p < 0.05$) log-fold changes in the abundances of bacterial species in G3 compared to G2. Positive log-fold change points out an increase in abundance in G3 compared to G2, while negative log-fold change points out a reduction in abundance.

In terms of markers of dysbiosis, FC is considered as the standard non-invasive marker for assessing disease activity in CD and has been shown to have clinical utility especially in monitoring disease activity, relapse, response to therapy and patient-reported outcomes in patients with CD^{34–36}. Thus, we tried to find an association between FC and dysbiosis. As previously described in another study³⁷, and in agreement with a recent study³⁸, we showed no link between the severity of dysbiosis and FC levels.

We therefore focused on microbiota as a putative marker for CD symptom severity. To our knowledge, our study is the first to link a progressive change of microbiota in CD to a worsening of the CD symptoms. The results of the PCA confirmed the idea of a progression of the disease from G1 to G3 and the first axis of variability might very well be considered as a novel informative “score” for the severity of the disease that is worth computing in medical studies.

It is well established that dysbiosis is key to CD. Here we found that there were “key signatures” of symptoms’ worsening. The first transition from G1 to G2 that triggers symptoms severity is characterized by the loss of the main anti-inflammatory SCFA producers (*Roseburia*, *Eubacterium*, *Subdoligranulum*, *Ruminococcus*) and increased pro-inflammatory bacteria such as *Proteus* and *Fingoldia*. These findings are in accordance with Neumann et al. and Zhang et al.^{39,40}. Neumann et al. showed for the first time *Fingoldia* as an inducer of inflammation due to the interaction with human neutrophils³⁹. *Proteus* has been recently shown to be a key factor in predicting disease relapse⁴⁰. The depletion of SCFA-producing bacteria is interesting in the context of these symptoms-microbiota interaction and the natural history of CD. Indeed, it has been shown that SCFAs promote anti-inflammatory T and B cell responses as well as an anti-inflammatory phenotype of intestinal macrophages^{41–46}. Finally, previous studies also showed that SCFAs/butyrate have inhibitory effects on inflammatory response, contributing to intestinal homeostasis and cancer protection^{47–51}.

Then, the second transition from G2 to G3, associated to a further worsening of the symptoms’ severity, is characterized by the increase of others pro-inflammatory bacteria (*Klebsiella*, *Pseudomonas*, *Salmonella*, *Acinetobacter*, *Hafnia*, *Staphylococcus*, *Enterococcus*, *Streptococcus*). With Quantitative Microbiome Profiling, in agreement with our study, Vieira-Silva et al. have also identified the same genera *Enterococcus*, *Escherichia*, *Fusobacterium*, *Streptococcus*, and *Veillonella* as biomarkers for clinical severity⁵². Precisely, *Fusobacterium* and *Veillonella* were associated in patients with higher gastrointestinal inflammation. *Enterococcus* was particularly linked to biliary obstruction severity.

The challenge remains to understand whether existing or future treatments might be able to stop or reverse dysbiosis progression, improving the prognosis and changing the natural history of CD. We believe that the knowledge of the sequence in microbiota changes we identified in this paper might provide further insight into personalized fecal microbiota transplantation (FMT) by providing a step-by-step remediation process. Indeed, in a very recent study, (FMT) was effective to maintain remission in CD patients⁵³. This link between microbiota and CD symptoms also strengthens the growing efforts regarding pre- and probiotic therapies. More specifically, our results suggest that SCFA production is associated with a restoration of intestinal homeostasis and sustained remission in CD patients. So far, probiotic treatments have not shown a significant effect in inducing or maintaining remission of active or quiescent CD, or in preventing relapse of CD after surgically-induced remission^{54,55}. However, probiotics evaluated in these studies were not SCFA-producing bacteria.

Interestingly, a recent study provided proof-of-concept evidence for the therapeutic potential of SCFAs-producing bacteria in CD. In CD patients, treatment with a mix of 6 SCFAs-producers (*Butyricoccus pulli-caecorum* 25-3T, *Faecalibacterium prausnitzii*, *Roseburia hominis*, *Roseburia inulinivorans*, *Anaerostipescaecae*, and *Eubacterium hallii*) improved butyrate production, colonization capacity in mucus and lumen-associated CD microbiota as well as epithelial barrier integrity⁵⁶. Such approaches may efficiently complement anti-TNF α therapy for reconstituting a healthy microbiome.

Conclusions

The purpose of the study was to better understand disease history, heterogeneity and to show the potential for machine learning to assist clinicians with personalized CD treatment⁵⁷. Our study confirms that unsupervised machine learning approaches are suited to characterize the gut dysbiosis and shows the association between this dysbiosis and symptom severity. Dysbiosis degree should be assessed along CD history to optimize CD management.

Data availability

The datasets analysed during the current study are publicly available: <https://doi.org/10.57745/CMF9FC>.

Received: 11 February 2022; Accepted: 4 November 2022

Published online: 19 November 2022

References

1. Dovrolis, N. *et al.* Gut microbial signatures underline complicated Crohn’s disease but vary between cohorts; an in silico approach. *Inflamm. Bowel Dis.* **25**, 217–225 (2019).
2. Lopez-Siles, M. *et al.* Mucosa-associated *Faecalibacterium prausnitzii* and *Escherichia coli* co-abundance can distinguish irritable bowel syndrome and inflammatory bowel disease phenotypes. *Int. J. Med. Microbiol. IJMM* **304**, 464–475 (2014).
3. Zuo, T. & Ng, S. C. The gut microbiota in the pathogenesis and therapeutics of inflammatory bowel disease. *Front. Microbiol.* **9**, 2247 (2018).
4. Lloyd-Price, J. *et al.* Multi-omics of the gut microbial ecosystem in inflammatory bowel diseases. *Nature* **569**, 655–662 (2019).
5. Moradkhani, A., Beckman, L. J. & Tabibian, J. H. Health-related quality of life in inflammatory bowel disease: Psychosocial, clinical, socioeconomic, and demographic predictors. *J. Crohns Colitis* **7**, 467–473 (2013).
6. Shah, S. C., Colombel, J.-F., Sands, B. E. & Narula, N. Systematic review with meta-analysis: Mucosal healing is associated with improved long-term outcomes in Crohn’s disease. *Aliment. Pharmacol. Ther.* **43**, 317–333 (2016).

7. Torres, J., Mehandru, S., Colombel, J.-F. & Peyrin-Biroulet, L. Crohn's disease. *Lancet Lond. Engl.* **389**, 1741–1755 (2017).
8. Thia, K. T., Sandborn, W. J., Harmsen, W. S., Zinsmeister, A. R. & Loftus, E. V. Risk factors associated with progression to intestinal complications of Crohn's disease in a population-based cohort. *Gastroenterology* **139**, 1147–1155 (2010).
9. Fiorino, G., Bonifacio, C., Peyrin-Biroulet, L. & Danese, S. Preventing collateral damage in Crohn's disease: The Lémann index. *J. Crohns Colitis* **10**, 495–500 (2016).
10. Vermeire, S., Schreiber, S., Sandborn, W. J., Dubois, C. & Rutgeerts, P. Correlation between the Crohn's disease activity and Harvey-Bradshaw indices in assessing Crohn's disease severity. *Clin. Gastroenterol. Hepatol. Off. Clin. Pract. J. Am. Gastroenterol. Assoc.* **8**, 357–363 (2010).
11. Klindworth, A. *et al.* Evaluation of general 16S ribosomal RNA gene PCR primers for classical and next-generation sequencing-based diversity studies. *Nucleic Acids Res.* **41**, e1 (2013).
12. Escudé, F. *et al.* FROGS: Find, rapidly, OTUs with galaxy solution. *Bioinform. Oxf. Engl.* **34**, 1287–1294 (2018).
13. Tsilimigras, M. C. B. & Fodor, A. A. Compositional data analysis of the microbiome: Fundamentals, tools, and challenges. *Ann. Epidemiol.* **26**, 330–335 (2016).
14. Mossotto, E. *et al.* Classification of paediatric inflammatory bowel disease using machine learning. *Sci. Rep.* **7**, 2427 (2017).
15. Virtanen, P. *et al.* SciPy 1.0: Fundamental algorithms for scientific computing in Python. *Nat. Methods* **17**, 261–272 (2020).
16. Ng, S. C. *et al.* Worldwide incidence and prevalence of inflammatory bowel disease in the 21st century: A systematic review of population-based studies. *Lancet Lond. Engl.* **390**, 2769–2778 (2017).
17. Piovani, D. *et al.* Environmental risk factors for inflammatory bowel diseases: An umbrella review of meta-analyses. *Gastroenterology* **157**, 647–659.e4 (2019).
18. Hansen, R. *et al.* Microbiota of de-novo pediatric IBD: Increased *Faecalibacterium prausnitzii* and reduced bacterial diversity in Crohn's but not in ulcerative colitis. *Am. J. Gastroenterol.* **107**, 1913–1922 (2012).
19. Manichanh, C. *et al.* Reduced diversity of faecal microbiota in Crohn's disease revealed by a metagenomic approach. *Gut* **55**, 205–211 (2006).
20. Mondot, S. *et al.* Highlighting new phylogenetic specificities of Crohn's disease microbiota. *Inflamm. Bowel Dis.* **17**, 185–192 (2011).
21. Sokol, H. *et al.* Fungal microbiota dysbiosis in IBD. *Gut* **66**, 1039–1048 (2017).
22. Pascal, V. *et al.* A microbial signature for Crohn's disease. *Gut* **66**, 813–822 (2017).
23. Forbes, J. D. *et al.* A comparative study of the gut microbiota in immune-mediated inflammatory diseases—does a common dysbiosis exist? *Microbiome* **6**, 221 (2018).
24. D'Haens, G. *et al.* Early combined immunosuppression or conventional management in patients with newly diagnosed Crohn's disease: An open randomised trial. *Lancet Lond. Engl.* **371**, 660–667 (2008).
25. Khanna, R. *et al.* Early combined immunosuppression for the management of Crohn's disease (REACT): A cluster randomised controlled trial. *Lancet Lond. Engl.* **386**, 1825–1834 (2015).
26. Piening, B. D. *et al.* Integrative personal omics profiles during periods of weight gain and loss. *Cell Syst.* **6**, 157–170.e8 (2018).
27. Zhou, W. *et al.* Longitudinal multi-omics of host-microbe dynamics in prediabetes. *Nature* **569**, 663–671 (2019).
28. Ghannam, R. B. & Techtman, S. M. Machine learning applications in microbial ecology, human microbiome studies, and environmental monitoring. *Comput. Struct. Biotechnol. J.* **19**, 1092–1107 (2021).
29. Kohli, A., Holzwanger, E. A. & Levy, A. N. Emerging use of artificial intelligence in inflammatory bowel disease. *World J. Gastroenterol.* **26**, 6923–6928 (2020).
30. Gevers, D. *et al.* The treatment-naïve microbiome in new-onset Crohn's disease. *Cell Host Microbe* **15**, 382–392 (2014).
31. Hofer, U. Microbiome: Bacterial imbalance in Crohn's disease. *Nat. Rev. Microbiol.* **12**, 312 (2014).
32. Yilmaz, B. *et al.* Microbial network disturbances in relapsing refractory Crohn's disease. *Nat. Med.* **25**, 323–336 (2019).
33. Ananthakrishnan, A. N. *et al.* Gut microbiome function predicts response to anti-integrin biologic therapy in inflammatory bowel diseases. *Cell Host Microbe* **21**, 603–610.e3 (2017).
34. Carroccio, A. *et al.* Diagnostic accuracy of fecal calprotectin assay in distinguishing organic causes of chronic diarrhea from irritable bowel syndrome: A prospective study in adults and children. *Clin. Chem.* **49**, 861–867 (2003).
35. Vermeire, S., Van Assche, G. & Rutgeerts, P. Laboratory markers in IBD: Useful, magic, or unnecessary toys? *Gut* **55**, 426–431 (2006).
36. Goutorbe, F. *et al.* Endoscopic factors influencing fecal calprotectin value in Crohn's disease. *J. Crohns Colitis* **9**, 1113–1119 (2015).
37. Rajca, S. *et al.* Alterations in the intestinal microbiome (dysbiosis) as a predictor of relapse after infliximab withdrawal in Crohn's disease. *Inflamm. Bowel Dis.* **20**, 978–986 (2014).
38. Buffet-Bataillon, S., Landreau, C., Siproudhis, L., Cattoir, V. & Bouguen, G. Bacterial gut dysbiosis is associated with Crohn's disease symptoms but not with elevated fecal calprotectin. *Clin. Res. Hepatol. Gastroenterol.* **45**, 101669 (2021).
39. Neumann, A., Björck, L. & Frick, I.-M. *Finegoldia magna*, an anaerobic Gram-positive bacterium of the normal human microbiota, induces inflammation by activating neutrophils. *Front. Microbiol.* **11**, 65 (2020).
40. Zhang, J. *et al.* Elucidation of *Proteus mirabilis* as a key bacterium in Crohn's disease inflammation. *Gastroenterology* **160**, 317–330.e11 (2021).
41. Smith, P. M. *et al.* The microbial metabolites, short-chain fatty acids, regulate colonic Treg cell homeostasis. *Science* **341**, 569–573 (2013).
42. Furusawa, Y. *et al.* Commensal microbe-derived butyrate induces the differentiation of colonic regulatory T cells. *Nature* **504**, 446–450 (2013).
43. Kim, M., Qie, Y., Park, J. & Kim, C. H. Gut microbial metabolites fuel host antibody responses. *Cell Host Microbe* **20**, 202–214 (2016).
44. Chang, P. V., Hao, L., Offermanns, S. & Medzhitov, R. The microbial metabolite butyrate regulates intestinal macrophage function via histone deacetylase inhibition. *Proc. Natl. Acad. Sci. USA* **111**, 2247–2252 (2014).
45. Wu, W. *et al.* Microbiota metabolite short-chain fatty acid acetate promotes intestinal IgA response to microbiota which is mediated by GPR43. *Mucosal Immunol.* **10**, 946–956 (2017).
46. Scott, N. A. *et al.* Antibiotics induce sustained dysregulation of intestinal T cell immunity by perturbing macrophage homeostasis. *Sci. Transl. Med.* **10**, eaa04755 (2018).
47. Riggs, M. G., Whittaker, R. G., Neumann, J. R. & Ingram, V. M. *n*-Butyrate causes histone modification in HeLa and friend erythroleukaemia cells. *Nature* **268**, 462–464 (1977).
48. Davie, J. R. Inhibition of histone deacetylase activity by butyrate. *J. Nutr.* **133**, 2485S–2493S (2003).
49. Matthews, G. M., Howarth, G. S. & Butler, R. N. Short-chain fatty acids induce apoptosis in colon cancer cells associated with changes to intracellular redox state and glucose metabolism. *Chemotherapy* **58**, 102–109 (2012).
50. Tang, Y., Chen, Y., Jiang, H. & Nie, D. Short-chain fatty acids induced autophagy serves as an adaptive strategy for retarding mitochondria-mediated apoptotic cell death. *Cell Death Differ.* **18**, 602–618 (2011).
51. Zhang, J. *et al.* Sodium butyrate induces endoplasmic reticulum stress and autophagy in colorectal cells: Implications for apoptosis. *PLoS ONE* **11**, e0147218 (2016).
52. Vieira-Silva, S. *et al.* Quantitative microbiome profiling disentangles inflammation- and bile duct obstruction-associated microbiota alterations across PSC/IBD diagnoses. *Nat. Microbiol.* **4**, 1826–1831 (2019).
53. Sokol, H. *et al.* Fecal microbiota transplantation to maintain remission in Crohn's disease: A pilot randomized controlled study. *Microbiome* **8**, 12 (2020).

54. Ganji-Arjenaki, M. & Rafeian-Kopaei, M. Probiotics are a good choice in remission of inflammatory bowel diseases: A meta analysis and systematic review. *J. Cell. Physiol.* **233**, 2091–2103 (2018).
55. Derwa, Y., Gracie, D. J., Hamlin, P. J. & Ford, A. C. Systematic review with meta-analysis: The efficacy of probiotics in inflammatory bowel disease. *Aliment. Pharmacol. Ther.* **46**, 389–400 (2017).
56. Geirnaert, A. *et al.* Butyrate-producing bacteria supplemented in vitro to Crohn's disease patient microbiota increased butyrate production and enhanced intestinal epithelial barrier integrity. *Sci. Rep.* **7**, 11450 (2017).
57. Allen, P. B., Gower-Rousseau, C., Danese, S. & Peyrin-Biroulet, L. Preventing disability in inflammatory bowel disease. *Ther. Adv. Gastroenterol.* **10**, 865–876 (2017).

Acknowledgements

We thank Maria Bernard (GABI, Toulouse) for her help in processing the FASTQ samples and her insights regarding FROGS.

Author contributions

S.B.B. and Y.L.C. designed the study. G.B. managed the clinical research. G.B. recruited patients and obtained the samples and clinical details. S.B.B. performed 16S rRNA sequencing of the microbiota. S.B.B. and M.B. performed the bioinformatic workflow for metataxonomic analysis. F.F. and Y.L.C. performed the data analysis. V.C. helped with the study realization. S.B.B., G.B., V.C. and Y.L.C. wrote the manuscript. The manuscript including the related data, figures, and tables has not been previously published and the manuscript is not under consideration elsewhere. All authors read and approved the final manuscript.

Competing interests

The authors declare no competing interests.

Additional information

Correspondence and requests for materials should be addressed to Y.C.

Reprints and permissions information is available at www.nature.com/reprints.

Publisher's note Springer Nature remains neutral with regard to jurisdictional claims in published maps and institutional affiliations.



Open Access This article is licensed under a Creative Commons Attribution 4.0 International License, which permits use, sharing, adaptation, distribution and reproduction in any medium or format, as long as you give appropriate credit to the original author(s) and the source, provide a link to the Creative Commons licence, and indicate if changes were made. The images or other third party material in this article are included in the article's Creative Commons licence, unless indicated otherwise in a credit line to the material. If material is not included in the article's Creative Commons licence and your intended use is not permitted by statutory regulation or exceeds the permitted use, you will need to obtain permission directly from the copyright holder. To view a copy of this licence, visit <http://creativecommons.org/licenses/by/4.0/>.

© The Author(s) 2022